Received: 9 August 2024 | Revised: 10 December 2024 | Accepted: 18 January 2025

DOI: 10.1002/mp.17666

DATASET ARTICLE

MEDICAL PHYSICS

A database of magnetic resonance imaging-transcranial ultrasound co-registration

Maryam Alizadeh[1] | **D. Louis Collins**[2,3,4] | **Marta Kersten-Oertel**[1,5] | **Yiming Xiao**[1,5]

[1]Department of Computer Science and Software Engineering, Concordia University, Montreal, Canada

[2]McConnell Brain Imaging Centre, Montreal Neurological Institute, McGill University, Montreal, Canada

[3]Department of Biomedical Engineering, McGill University, Montreal, Canada

[4]Department of Neurology and Neurosurgery, McGill University, Montreal, Canada

[5]School of Health, Concordia University, Montreal, Canada

Correspondence
Maryam Alizadeh, Department of Computer Science and Software Engineering, Concordia University, Montreal, H3G 1M8, Canada.
Email: maryam.alizadeh@concordia.ca

Funding information
New Frontiers in Research Fund, Grant/Award Number: NFRFE-2020-00241; Concordia University Horizon Postdoctoral Fellowship; Fonds de recherche du Québec-Santé Junior 1 and 2 Research Scholar program, and Parkinson Québec

Abstract

Purpose: As a portable and cost-effective imaging modality with better accessibility than Magnetic Resonance Imaging (MRI), transcranial sonography (TCS) has demonstrated its flexibility and potential utility in various clinical diagnostic applications, including Parkinson's disease and cerebrovascular conditions. To better understand the information in TCS for data analysis and acquisition, MRI can provide guidance for efficient imaging with neuronavigation systems and the confirmation of disease-related abnormality. In these cases, MRI-TCS co-registration is crucial, but relevant public databases are scarce to help develop the related algorithms and software systems.

Acquisition and validation methods: This dataset comprises manually registered MRI and transcranial ultrasound volumes from eight healthy subjects. Three raters manually registered each subject's scans, based on visual inspection of image feature correspondence. Average transformation matrices were computed from all raters' alignments for each subject. Inter- and intra-rater variability in the transformations conducted by raters are presented to validate the accuracy and consistency of manual registration. In addition, a population-averaged MRI brain vascular atlas is provided to facilitate the development of computer-assisted TCS acquisition software.

Data format and usage notes: The dataset is provided in both NIFTI and MINC formats and is publicly available on the OSF data repository: https://osf.io/zdcjb/.

Potential applications: This dataset provides the first public resource for the development and assessment of MRI-TCS registration with manual ground truths, as well as resources for establishing neuronavigation software in data acquisition and analysis of TCS. These technical advancements could greatly boost TCS as an imaging tool for clinical applications in the diagnosis of neurological conditions such as Parkinson's disease and cerebrovascular disorders.

KEYWORDS
MRI, multi-modal image registration, transcranial ultrasound

1 | INTRODUCTION

Magnetic Resonance Imaging (MRI) is a widely utilized medical imaging technique due to its capacity to provide detailed and precise visual data crucial for diagnosis, treatment planning, and study of diseases. However, MRI scanning is often costly and time-consuming with limited accessibility in some regions. In contrast, ultrasound (US) offers a portable, cost-effective, and more accessible alternative that facilitates real-time imaging without interrupting the medical procedure. Nevertheless, ultrasound's imaging capabilities are characterized by lower

resolution, unintuitive image contrast,[1] and non-standard imaging planes, which pose challenges in interpretation that relies on operator's experience.[2] Thickness of the skull's acoustic window can also impact the quality of the acquired US signal, occasionally rendering it unusable, in 5-20% of cases, due to excessive skull thickness.[3,4] Therefore, fusing these two modalities could well complement their strengths. This necessitates the accurate inter-modal registration. However, discrepancies in image features, anatomical variability, image artifacts, and tissue motion can complicate the registration process.[5–7] While manual registration is laborious and susceptible to the operator's expertise, more efficient and robust automatic registration algorithms still require further investigation.

In neurosurgery and clinical diagnosis, transcranial sonography (TCS) can image neuroanatomical structures through the intact skull, making it particularly valuable for imaging neurovascular health and assessing neuroanatomy in applications, such as ventricular assessments during the placement of external ventricular drains[8,9] and differential diagnosis of neurological conditions, such as Parkinson's disease.[10–15] Similarly, TCS can greatly benefit from fusion with MRI data to better understand the acquired signals so that we can further enhance its clinical potential. To date, only a few public multimodality datasets exist focusing on MRI-US registration. Natarajan et al.[16] presents a dataset comprising preoperative MRI scans paired with 3D transrectal prostate US, specifically collected for image-guided biopsy procedures. In neurosurgery, BITE,[17] RESECT[18,19] and ReMIND[20] are examples of available datasets, offering preoperative MRI alongside 3D intra-operative US scans of patients undergoing brain tumor resection to address the challenges of brain shift during surgical procedures. However, to the best of the authors' knowledge, similar datasets for registered MRI vs. transcranial US are not available, and this dataset is the first of its kind.

In this paper, we introduce a dataset of MRI versus TCS co-registration for the development of relevant multi-modal registration algorithms. These algorithms can greatly facilitate the interpretation of TCS and the confirmation of its findings to further enhance its precision and value for diagnostic and surgical applications. Our dataset comprises registered MRI and 3D volumes of TCS scans from 8 healthy subjects, along with their associated transformations. Examples of the registered and superimposed MRI and US images are shown in Figure 1b, c, and d. We also incorporate a probabilistic blood vessel atlas into the dataset, which, thanks to the relatively consistent spatial arrangement of major cerebral vascular branches, provides another valuable tool for interpreting transcranial US scans. This can be leveraged in the development of computer-assisted TCS acquisition software and algorithms, similar to that proposed by Xiao et al.[21] which used the atlas to guide transcranial Doppler (TCD) US examinations. Furthermore, the atlas can be employed in other computer-assisted diagnostic and surgical applications, where subject-specific CT/MRI angiographies are difficult to obtain.

2 | METHODS

2.1 | Data acquisition

The described dataset comprises registered MRI and 3D volumes of transcranial US scans acquired from eight healthy subjects (three females, age = 33 ± 12 yo) upon informed consent. It also includes the transformation matrices essential for the alignment of MRI and US scans. The whole-head MRI scans were acquired using a 3T Siemens Trio Tim scanner (Siemens, Erlangen, Germany) with a T1w MP-RAGE sequence (echo time = 2.98 ms, repetition time = 2300 ms, inversion time = 900 ms, flip angle = 9∘, BW = 238 Hz/px, resolution = $1 \times 1 \times 1 mm^3$). This MRI sequence has low geometric distortion, so no distortion correction was performed. In addition, we provide the MRI data without bias field correction. The TCS data were acquired using the Toshiba Aplio XG scanner with the PST-25BT transducer (2-4MHz). During data acquisition, the transducer was spatially tracked using an optical tracking system. The tracked 2D B-mode transcranial US images were obtained from left and right temporal bone windows of the subjects at an imaging depth of 15 cm, from which two 3D TCS volumes (left and right) were constructed in the resolution of $1 \times 1 \times 1 mm^3$ for each subject. The data collection was approved by the ethics committee of the Montreal Neurological Institute (Montreal, Canada).

Manual MRI scans and TCS volumes co-registration was performed by three raters, who are experienced with neuroanatomy. From the TCS acquisition, the MRI and TCS scans for each subject were initially roughly aligned through facial landmark-based (nose bridge, left and right medial canthi, left and right lateral canthi, left and right tragi, and left and right tragus valleys) registration and optical tracking.[21] Based on the initial alignment, further manual rigid registration was performed with the open-source IBIS (Intraoperative Brain Imaging System) neuronavigation platform.[22] While visually inspecting the image feature alignment in real-time, the six parameters of rigid transformation were manually adjusted via a control panel within the software. One of the three raters conducted the alignments twice in two separate sessions with one week apart to assess the intra-rater variability.

The silver ground truth transformation matrices for MRI versus TCS registration, derived from three raters' manual alignments, were computed for all subjects. First, a grid of landmarks with $10 \times 10 \times 10$ mm^3 spacing was established within the brain region of each MRI

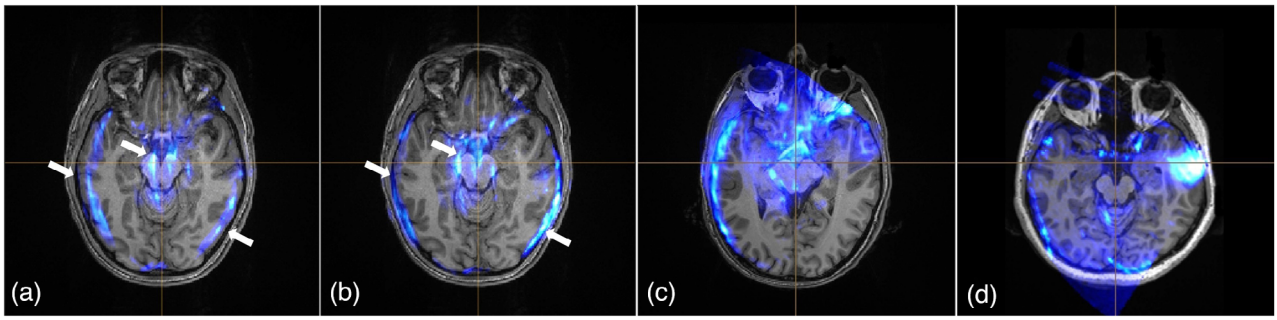

FIGURE 1 Examples of superimposed MRI and transcranial US scans; (a) and (b) show the before and after application of the silver-ground truth alignment, respectively. White arrows point to the brainstem and the edge of the brain where MRI and TCS images are successfully aligned after the registration. Additionally, (c) and (d) illustrate the transcranial ultrasound signal variability from two additional subjects. MRI, magnetic resonance imaging; TCS, Transcranial sonography; US, ultrasound.

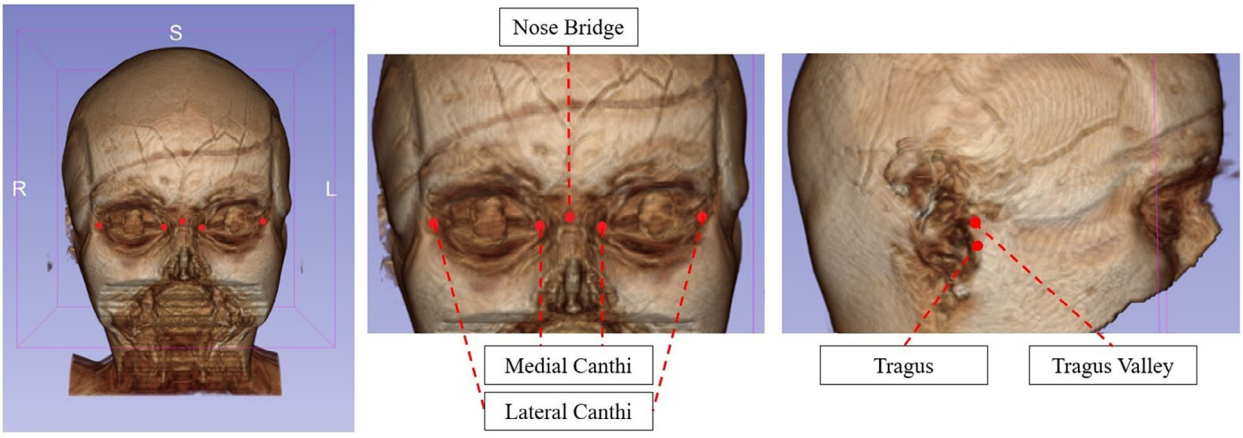

FIGURE 2 Front and side views of defaced MRI volume of one subject and the facial landmarks denoted by the red dots. MRI, magnetic resonance imaging.

scan. Then, these landmarks were rigidly transformed to the space of the TCS volume based on the transformation matrix from manual alignment. Three sets of transformed landmarks were obtained from three raters' registrations and an averaged spatial coordinate for each landmark was obtained. Finally, the silver ground truth registration matrix for each subject was created based on landmark-based rigid alignment between the MRI landmarks and the corresponding, averaged ones in the TCS space. An example of MRI and TCS pair, before and after the silver ground truth alignment is depicted in Figure 1a,b.

Besides removing all identifying information from the image headers of the MRI and TCS, further anonymization of MRI volumes was conducted by manual defacing using 3DSlicer[23] to best preserve the facial landmarks for computer-assisted TCS acquisition.[21] Specifically, we removed the ear lobes, the central portion of the eyes, and the lower part of the face, while conscientiously maintaining the integrity of the regions that contain the facial landmarks. Figure 2 illustrates an example of the defaced MRI volume for one subject, along with the corresponding facial landmarks.

In addition to the individual MRI and TCS pairs, we also include a population-averaged, unbiased head atlas, comprising a T1w MRI template and a probabilistic blood vessel map, with the construction procedure detailed in our previous study.[21] Specifically, the T1w head MRI template was constructed in the ICBM152 space using group-wise registration[24] from 20 healthy adult subjects. Additionally, the corresponding facial landmarks of the template were also created. The probabilistic blood vessel map was derived from MR angiographies (MRAs), which were first segmented with a Frangi vesselness filter[25] and then averaged from all subjects after group-wise registration. Figure 3 depicts axial and sagittal views of the MRI template with the probabilistic blood vessel map and the 3D rendering of the head template with the average facial landmarks.

2.2 | Data validation

To assess the accuracy of the manual registration of MRI and TCS scans, we measured the inter- and intra-rater variability. To ensure a more detailed and accurate

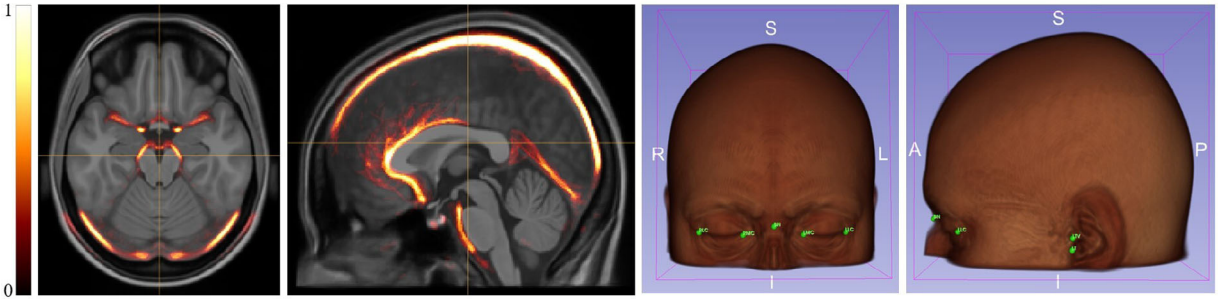

FIGURE 3 Axial and sagittal views of the MRI template superimposed by the average vessel map, highlighted using the heat colormap, and the 3D volume of head template with average facial landmarks. MRI, magnetic resonance imaging.

TABLE 1 Absolute errors (mean ± std) for individual elements of rigid transformation representing the inter- and intra-rater variability.

		Inter-rater variability			Intra-rater variability
		Rater I	Rater II	Rater III	Rater II-1st and 2nd sets
Translation (*mm*)	*X* axis	0.78 ± 0.93	1.06 ± 0.65	1.73 ± 0.85	0.94 ± 0.77
	Y axis	0.95 ± 0.69	1.16 ± 0.78	1.51 ± 0.87	1.18 ± 1.04
	Z axis	1.72 ± 0.78	1.52 ± 1.02	1.63 ± 0.72	0.81 ± 1.10
Rotation (*degree*)	*X* axis	0.82 ± 2.12	0.41 ± 1.02	0.41 ± 1.02	0.18 ± 0.75
	Y axis	2.93 ± 2.05	1.54 ± 1.06	1.51 ± 1.06	0.25 ± 0.77
	Z axis	1.37 ± 1.31	0.79 ± 0.81	0.77 ± 0.76	0.56 ± 1.41

TABLE 2 Landmark-based inter- and intra-rater variability assessments (mean ± std).

	Inter-rater variability			Intra-rater variability
	Rater I	Rater II	Rater III	Rater II-1st and 2nd sets
Average distance(*mm*) (mean ± sd)	2.52 ± 0.68	1.95 ± 0.48	2.12 ± 0.53	1.54 ± 0.87

analysis, the transformation matrices were decomposed into individual translation and rotation parameters. Additionally, matrix elements were compared separately for each of *x*-, *y*-, and *z*-axes to facilitate a thorough examination of discrepancies in registrations obtained by different raters. The mean and standard deviation of absolute error values of alignments conducted by three different raters from the silver ground truth, as well as alignments performed by Rater II in two separate sessions, were calculated and reported as inter- and intra-rater variability, respectively. Table 1 presents the error values representing these variability parameters.

To evaluate inter- and intra-rater variability using an alternative method, we employed the grid of landmarks previously mentioned in Section 2.1 to obtain distance measures, which are more relevant to image registration tasks. As for inter-rater variability, we calculated and reported the average distance between each rater's transformed grid of landmarks and the average of the three sets of transformed landmarks in the TCS space of a subject. For intra-rater variability, we computed the average distance between two sets of deformed landmarks in the TCS space from two separate transformations performed by Rater II. The landmark-based inter- and intra-rater variability assessments are shown in Table 2.

2.3 | Data format and usage notes

The described dataset includes MRI scans and 3D volumes of TCS obtained from left and right temporal bone windows from eight healthy subjects. The data is available in both NIFTI and MINC formats. For each subject, the dataset provides one T1w MR image and a pair of left and right 3D transcranial US scans. Additionally, the averaged transformation matrices from three raters' alignments are included, along with facial landmark coordinates for each subject, available in both .FCSV and MNI tag files, compatible with NIFTI and MINC formats, respectively.

Besides individual MRI-TCS scans, the population-averaged "Head Atlas" includes a T1w MRI template and an average vessel map in NIFTI and MINC formats, and the corresponding facial landmarks in .FCSV and MNI tag file formats. The dataset is made available on the Open Science Framework (OSF) data repository https://osf.io/zdcjb/.

3 | DISCUSSION

A dataset of registered MRI and 3D volumes of transcranial US scans, as well as a population-averaged head atlas are provided in this work. The manual registration process performed by three raters yielded accurate registration of MRI and TCS scans in consideration of the characteristics of the imaging modalities. The evaluation of inter- and intra-rater variability provides a comprehensive understanding of the reliability and consistency of the manual registration process within the dataset.

The utility of this dataset extends across two primary dimensions: technical and clinical. On the technical side, one major application lies in the evaluation of registration algorithms. The precise alignment of MRI and US images is imperative for leveraging the combined strengths of both modalities. This dataset offers reliable ground truths to facilitate the assessment of registration algorithms' performance. Moreover, the provided alignment can be exploited for image processing tasks, such as the development of image fusion techniques,[26] where MRI and US images are merged to enhance data visualization. The dataset may further lend itself to training machine learning models for pattern recognition, harnessing the complementary information from both imaging modalities.[7,27] With the advancement and increased use of transcranial US, this dataset can also be used in the development of techniques facilitating the interpretation of the US.[28,29] On the clinical front, the dataset holds significant potential to facilitate the development of diagnostic techniques targeting diseases affecting the structural, shape, and size aspects of the brain, such as movement disorders.[30–32] The accessibility of US scans opens avenues for early diagnosis and subsequent treatment, potentially leading to improved patient outcomes. Additionally, the dataset can contribute to the development of systems catering to pre-operative planning[33] and intraoperative image-guidance in neurosurgical procedures, such as cannula insertions and ventriculostomy.[8,9] It can also be used in developing software systems for guided TCS examination, facilitating both the acquisition and interpretation of US data.[21] The integration of real-time US with pre-operative MRI data and the population-averaged head template provides enhanced, real-time guidance, exemplifying the dataset's relevance in advancing clinical applications for neurosurgery.

Nevertheless, there are limitations that need to be considered. To help define the co-registration ground truths, we obtained the averaged manual alignment from three raters as absolute ground truths are not feasible to acquire. Several factors can complicate manual registration, including the coarse features of US, navigation of volumetric data based on slice-wise 2D displays, individual perceptual differences in image features, and distinctions between the feature characteristics between MRI and transcranial US. However, intra- and inter-rater variability assessments have indicated good reliability in consideration of these factors. Furthermore, the variability in skull thickness among subjects, poses challenges to good TCS image quality, resulting in the exclusion of transcranial US data of two subjects from the original data acquisition due to poor tissue contrast. Also, the dataset's sample size is limited; however, our unique dataset provides the opportunity to inspect TCS-related acquisition and analysis further, and we intend to enrich the repository with additional subjects in the future.

4 | CONCLUSION

This work introduces a novel dataset of registered MRI and TCS scans, along with a probabilistic blood vessel atlas. It provides reliable ground truths that can be used to develop and evaluate multimodal registration techniques, as well as image fusion and machine learning algorithms. These potential methodological developments can facilitate the diagnosis of neurodegenerative diseases and neurosurgical planning. Overall, the presented dataset serves as a valuable resource for advancing TCS research and its clinical applications.

ACKNOWLEDGMENTS

This work has been supported by New Frontiers in Research Fund (NFRF) (fund number: NFRFE-2020-00241), Concordia University Horizon Postdoctoral Fellowship program, the Fonds de recherche du Québec-Santé Junior 1 and 2 Research Scholar program, and Parkinson Québec.

CONFLICT OF INTEREST STATEMENT

The authors declare no conflicts of interest.

REFERENCES

1. Abhisheka B, Biswas SK, Purkayastha B, Das D, Escargueil A. Recent trend in medical imaging modalities and their applications in disease diagnosis: a review. *Multimed Tools Appl*. 2023;83:43035–43070.
2. Downey DB, Fenster A, Williams JC. Clinical utility of three-dimensional US. *Radiographics*. 2000;20:559–571.
3. Rowbotham SK, Mole CG, Tieppo D, Blaszkowska M, Cordner SM, Blau S. Average thickness of the bones of the human neurocranium: development of reference measurements to assist with blunt force trauma interpretations. *Int J Legal Med*. 2023;137:195–213.
4. Kwon JH, Kim JS, Kang DW, Bae KS, Kwon SU. The thickness and texture of temporal bone in brain CT predict acoustic window failure of transcranial Doppler. *J. Neuroimaging*. 2006;16:347–352.
5. Hajnal JV, Hill DL. *Medical Image Registration*. CRC Press; 2001.
6. Alam F, Rahman SU. Challenges and solutions in multimodal medical image subregion detection and registration. *J. Med. Imaging Radiat. Sci.* 2019;50:24–30.
7. Xiao Y, Rivaz H, Chabanas M, et al. Evaluation of MRI to ultrasound registration methods for brain shift correction: the CuRIOUS2018 challenge. *IEEE Trans Med Imaging*. 2019;39:777–786.

8. Wilson TJ, Stetler WR, Al-Holou WN, Sullivan SE. Comparison of the accuracy of ventricular catheter placement using freehand placement, ultrasonic guidance, and stereotactic neuronavigation. *J Neurosurg*. 2013;119:66–70.
9. Unal T, Dolas I, Sahin D, et al. Intraoperative ultrasound-guided ventricular cannulation in patients with normal-sized ventricles. *Neurochirurgie*. 2023;69:101463.
10. Gaenslen A, Unmuth B, Godau J, et al. The specificity and sensitivity of transcranial ultrasound in the differential diagnosis of Parkinson's disease: a prospective blinded study. *The Lancet Neurol*. 2008;7:417–424.
11. Kang H, Wang X, Sun Y, et al. Automatic transcranial sonography-based classification of parkinson's disease using a novel dual-channel CNXV2-DANet. *Bioengineering*. 2024;11:889.
12. Ma X, Li T, Du L, Han T. Application and progress of transcranial substantial ultrasound in Parkinson's disease. *Front Neurol*. 2022;13:1091895.
13. Chen S, Shi Y, Wan L, et al. Attention-enhanced dilated convolution for Parkinson's disease detection using transcranial sonography. *Biomed Eng Online*. 2024;23:76.
14. Favaretto S, Walter U, Baracchini C, Cagnin A. Transcranial sonography in neurodegenerative diseases with cognitive decline. *J Alzheimers Dis*. 2018;61:29–40.
15. Wen Y, Zhou H, Xia M, Liu Q, Quan H, Fang L. Differentiating progressive supranuclear palsy from other movement disorders using transcranial sonography: a systematic review and meta-analysis. *Neurol Sci*. 2024;45:455–465.
16. Natarajan S, Priester A, Margolis D, Huang J, Marks L. Prostate MRI and ultrasound with pathology and coordinates of tracked biopsy (prostate-MRI-US-biopsy). *Cancer Imaging Arch*. 2020;10:7937.
17. Mercier L, Del Maestro RF, Petrecca K, Araujo D, Haegelen C, Collins DL. Online database of clinical MR and ultrasound images of brain tumors. *Med Phys*. 2012;39:3253–3261.
18. Xiao Y, Fortin M, Unsgård G, Rivaz H, Reinertsen I. REtroSpective Evaluation of Cerebral Tumors (RESECT): A clinical database of pre-operative MRI and intra-operative ultrasound in low-grade glioma surgeries. *Med Phys*. 2017;44:3875–3882.
19. Behboodi B, Carton FX, Chabanas M, et al. RESECT-SEG: Open access annotations of intra-operative brain tumor ultrasound images. *arXiv preprint arXiv:2207.07494* (2022). https://doi.org/10.48550/arXiv.2207.07494
20. Juvekar P, Dorent R., Kögl F., et al. ReMIND: The Brain Resection Multimodal Imaging Database. *Sci Data* 2024;11:494. https://doi.org/10.1038/s41597-024-03295-z
21. Xiao Y, Drouin S, Gerard IJ, et al. An augmented-reality system prototype for guiding transcranial Doppler ultrasound examination. *Multimed Tools Appl*. 2018;77:27789–27805.
22. Drouin S, Kochanowska A, Kersten-Oertel M, et al. IBIS: an OR ready open-source platform for image-guided neurosurgery. *Int J Comput Assist Radiol Surg*. 2017;12:363–378.
23. Fedorov A, Beichel R, Kalpathy-Cramer J, et al. 3D Slicer as an image computing platform for the Quantitative Imaging Network. *Magn Reson Imaging*. 2012;30:1323–1341.
24. Fonov V, Evans AC, Botteron KN, et al. Unbiased average age-appropriate atlases for pediatric studies. *Neuroimage*. 2011;54:313–327.
25. Frangi AF, Niessen WJ, Vincken KL, Viergever MA. Multiscale vessel enhancement filtering, In: Medical Image Computing and Computer-Assisted Intervention–MICCAI'98. First International Conference Cambridge, MA, USA, October 11–13, 1998. Springer; 1998:130–137.
26. Lang J, McClure TD, Margolis DJ. MRI–ultrasound fused approach for prostate biopsy–how it is performed. *Cancers*. 2024;16:1424.
27. Hering A, et al. Learn2Reg: comprehensive multi-task medical image registration challenge, dataset and evaluation in the era of deep learning. *IEEE Trans Med Imaging*. 2022;42:697–712.
28. Lindseth F, Kaspersen JH, Ommedal S, et al. Multimodal image fusion in ultrasound-based neuronavigation: improving overview and interpretation by integrating preoperative MRI with intraoperative 3D ultrasound. *Comput Aided Surg*. 2003;8:49–69.
29. Rasmussen IA, Lindseth F, Rygh OM, et al. Functional neuronavigation combined with intra-operative 3D ultrasound: initial experiences during surgical resections close to eloquent brain areas and future directions in automatic brain shift compensation of preoperative data. *Acta Neurochir*. 2007;149:365–378.
30. Brooks DJ. Imaging approaches to Parkinson disease. *J Nucl Med*. 2010;51:596–609.
31. Pauly O, Ahmadi SA, Plate A, Boetzel K, Navab N. Detection of substantia nigra echogenicities in 3D transcranial ultrasound for early diagnosis of Parkinson disease. *Med Image Comput Comput Assist Interv*. 2012:15:443–450.
32. Yilmaz R, Pilotto A, Roeben B, et al. Structural ultrasound of the medial temporal lobe in Alzheimer's disease. *Ultraschall Med*. 2017;38:294–300.
33. De Rosa A, Guizzardi G, Moncada M, et al. Ultrasound-oriented surgical planning ("UOSP") for intracranial lesions: a systematic integration to the standard preoperative planning. *World Neurosurg*. 2023;170:e766–e776.

How to cite this article: Alizadeh M, Collins DL, Kersten-Oertel M, Xiao Y. A database of magnetic resonance imaging-transcranial ultrasound co-registration. *Med Phys*. 2025;52:3481–3486. https://doi.org/10.1002/mp.17666